PROCEEDINGS OF SCIENCE

Constraining the fireball scenario of GRB afterglows with GROND and multi-wavelength data.

K. Varela, H. van Eerten, J. Greiner, P. Schady.
Max-Planck-Institut für Extraterrestrische Physik, Giessenbachstraße, 85748, Garching, Germany
E-mail: kvarela@mpe.mpg.de, hveerten@mpe.mpg.de, jcg@mpe.mpg.de, pschady@mpe.mpg.de

We performed an analysis of the multi-epoch broad-band observations of the GRB 121024A afterglow covering the full range from radio to X-rays. From the temporal and spectral evolution of the afterglow we set constraints on the micro-physical and dynamical parameters describing the physics of the afterglow. We tested both a jet break scenario and an energy injection model for the interpretation of the break in the light curve. The jet break model has been suggested by Wiersema et al., based on the linear and circular polarisation detections for this burst. The final values for the micro-physical and dynamical parameters in this model are physically plausible. However, it requires a hard distribution for the shock-accelerated electron energies, an extremely low value for the cooling break frequency, a non-spreading jet and an extreme prompt emission efficiency. The energy injection model avoids the unusual requirements of the jet break model but it gives some atypical values for the micro-physical and dynamical parameters.

Swift: 10 Years of Discovery,
2-5 December 2014
La Sapienza University, Rome, Italy

© Copyright owned by the author(s) under the terms of the Creative Commons Attribution-NonCommercial-ShareAlike Licence.

1. Introduction

In the standard GRB afterglow model [1], the observed emission is associated with synchrotron radiation from accelerated electrons. The observed spectrum has 3 characteristic breaks: the cooling frequency ν_c, the synchrotron injection frequency ν_m and the self-absorption frequency ν_{sa}. Each one yields specific and correlated constraints on the physical processes in the relativistic outflow. These processes are described by 3 micro-physical parameters (i.e. fraction of energy in the electrons ε_e and in the magnetic field ε_B, power-law index of the non-thermal electron population p) and 3 dynamical parameters (i.e. isotropic equivalent energy E_{iso}, circumburst density profile $n = Ar^{-k}$ with A a constant and r the radius, half-opening angle θ_0). Here, we present the analysis of the simultaneous multi-wavelength observations of GRB 121024A. It was followed up by different instruments in wavelengths from radio to X-rays during several days, and has a redshift z = 2.30 measured by the X-shooter spectrograph at the Very Large Telescope (VLT) [2]. From these simultaneous broad-band observations, we derive constraints on the micro-physical and dynamical parameters of the GRB afterglow. This burst is well known as the first one for which linear and circular optical polarisations have been observed that were claimed to cover a jet break [3].On the other hand a prolonged energy injection model avoids the main issues of the jet break scenario but gives atypical values for some of the derived parameters. Here, we present both scenarios.

2. Observations and data reduction

Swift X-ray Telescope (XRT): On October 24th 2012 at 02:56:12 UT the Swift Burst Alert Telescope (BAT) triggered and located GRB 121024A [4]. XRT slewed immediately to the burst and the observations started 93 sec after the trigger. The Swift/XRT light curve and spectra data were obtained from the XRT repository [5]. The measured energy in the prompt emission is $E^{\gamma}_{iso} = 8.4^{+2.6}_{-2.2} \times 10^{52}$ erg [6].

The Gamma-Ray burst Optical Near-infrared Detector - GROND [7] started observations of the GRB field 2.96 hours after the Swift trigger [8] and continued for the next 3.8 hours. The afterglow was detected at RA(J2000) = 04:41:53.30 and Dec(J2000) = -12:17:26.5 with an uncertainty of $0\farcs4$ in each coordinate in all the 7 bands $g'r'i'z'JHK_s$. Imaging of the field of GRB 121024A continued on the 2nd, 3rd, 4th, 16th and 17th night after the burst. The optical/NIR data was reduced using standard IRAF tasks [9]. The optical magnitudes were calibrated against secondary stars in the GRB field. The NIR magnitudes were calibrated against the Two Micron Sky Survey -2MASS- [10] catalogue stars in the field of the GRB.

The Large APEX Bolometer Camera LABOCA [11] was triggered on October 24th 2012[1]. Two observations at a frequency of 345 GHz with a band width of 60 GHz were performed. The first one started 19.8 ks after the GRB and the second was at a mid-time of 109.0 ks after the trigger. During both days, observations were taken in mapping and in on-off mode. There was no detection in either of both nights. The upper limits are 3.6 mJy beam^{-1} and 10.4 mJy beam^{-1} for the 1st and 2nd nights, respectively.

Millimeter and radio observations: The following values published in the literature are used in the analysis of the complete broad-band energy spectrum: The Combined Array for Research in

[1]Based on observations collected during Max-Planck time at the Atacama Pathfinder Experiment (APEX) under proposal M0005-90.

Millimeter-wave Astronomy (CARMA) started observations of the field of GRB 121024A $\sim$ 120.9 ks after the BAT trigger at a mean frequency of $\sim$ 85 GHz (3mm) [12]. A mm counterpart was detected with a flux of 1.0 ± 0.3 mJy. The Very Large Array (VLA) started observations of the field of GRB 121024A $\sim$ 109.0 ks after the trigger. They were performed using the K, C and X bands. A radio counterpart with flux of 0.10 ± 0.03 mJy was detected at frequency of 22 GHz [13].

3. Results

To study the temporal evolution, we first perform a combined fit using XRT and GROND data using a smoothly broken power-law with host contribution. The best fit reveals an achromatic break with slope going from $\alpha_{\rm pre} = -0.85 \pm 0.04$ to $\alpha_{\rm post} = -1.47 \pm 0.04$, smoothness sm $= 1.7 \pm 0.3$ and break time $t_{\rm b} = 49.8 \pm 5.1$ ks.

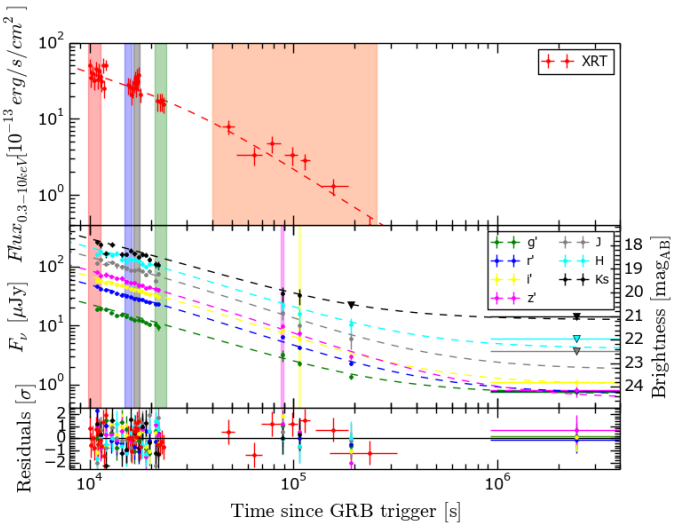

Figure 1: Light curve of the afterglow of GRB 121024A. **Top**: XRT light curve from the XRT repository. **Bottom**: GROND light curve $g'r'i'z'JHK_{\rm s}$. The epochs used for the spectral analysis are highlighted with the vertical lines.

To test for spectral evolution, we first use X-ray and optical/NIR measurements at 6 different epochs (see Fig.2a). The best fitting profile is a power-law with $\beta = 0.86 \pm 0.02$, showing no evidence for spectral evolution. There are two possible scenarios that can explain the observations. On one hand, we have $\nu_{\rm NIR} > \nu_{\rm c}$ with $p = 1.73 \pm 0.03$. This is a flat electron spectrum with the break in the light curve associated with a jet break. On the other hand, we obtain $\nu_{\rm c} > \nu_{\rm x-rays}$ with $p = 2.73 \pm 0.03$. In this case, the break in the light curve is the end of the energy injection phase in a stellar-wind type environment.

Now, we proceed to used the broad-band observations (Fig. 2b). For the SED at t=19.8 ks the APEX upper limit implies a break between APEX and NIR bands. This break is associated with $\nu_{\rm c}$ in the jet break scenario and with $\nu_{\rm m}$ in the energy injection scenario. For the SED at t=109.0 ks, the CARMA data point requires at least one break between this wavelength and the NIR bands and the EVLA data point implies a break between this wavelength and the CARMA wavelength. For the energy injection scenario, this break is associated with $\nu_{\rm sa}$. We analyse this scenario for ISM, wind and a generic density profile with slope 1.1. For the jet break scenario, we have two breaks, associated with $\nu_{\rm sa}$ and $\nu_{\rm m}$. In this scenario, $\nu_{\rm m}$ can be above or below $\nu_{\rm sa}$. We present both spectral regimes. The results for the parameters are presented in Table 1, where GS [14] and

DC [15] two different jet break scenarios for $p < 2$. The models presented here are those that were not ruled out by the closure relations.

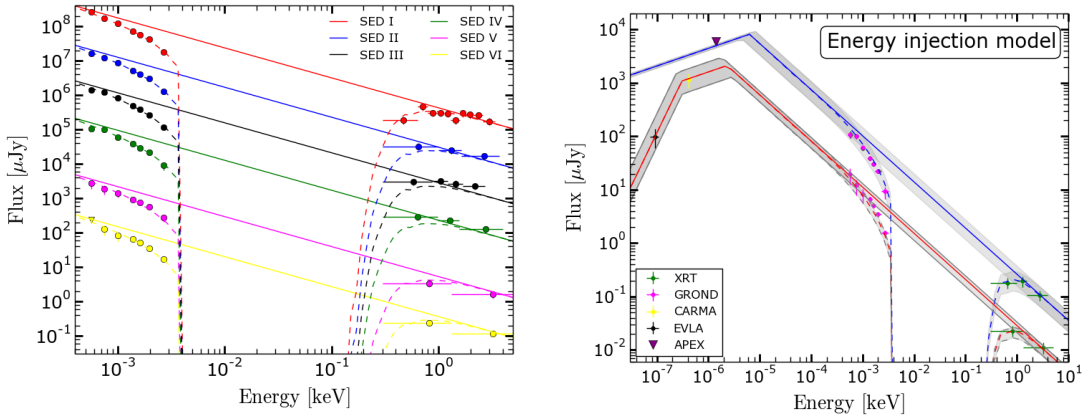

(a) SED for combined XRT and GROND data.

(b) SED for the energy injection model.

Figure 2: Left: Spectral energy distribution for the 6 SED highlighted in Fig.1. SEDs I - IV are from data before the observed break in the light curve. SEDs V - VI are from data taken after the break. The SEDs are scaled with arbitrary factor for clarity in the plot. **Right**: The red line corresponds to the SED at $t = 19.8$ ks. The green line is the SED at $t = 109.0$ ks. EVLA, CARMA, GROND and XRT data are included. We measured ν_{sa} and ν_m for the slow cooling regime when $\nu_c > \nu_{x-ray}$

Description	$\bar{\varepsilon}_e$	ε_B	A_* , n_0	θ_0 [rad]	$E_{iso,52}$[erg]	η
GS scenario where $p = 1.73 \pm 0.03$						
$\nu_{sa} < \nu_m$	$1.9^{+1.1}_{-0.8} \cdot 10^{-2}$	$2.2^{+0.6}_{-0.3} \cdot 10^{-2}$	$1.4^{+1.2}_{-0.8}$	$2.9^{+0.3}_{-0.4} \cdot 10^{-1}$	$1.7^{+0.3}_{-0.3} \cdot 10^{-1}$	$98^{+3}_{-3}\%$
$\nu_m < \nu_{sa}$	$< 8.8 \cdot 10^{-4}$	$< 8.3 \cdot 10^{-2}$	> 0.8	$> 1.2 \cdot 10^{-1}$	> 3.4	$< 71\%$
DC scenario where $p = 1.73 \pm 0.03$						
$\nu_{sa} < \nu_m$	$79.9^{14.1}_{6.3} \cdot 10^{-2}$	$5.0^{+0.2}_{-0.1} \cdot 10^{-3}$	$3.1^{+0.2}_{-0.1}$	$3.5^{+0.2}_{-0.2} \cdot 10^{-2}$	$1.9^{+0.7}_{-0.6} \cdot 10^{-2}$	$98^{+7}_{-6}\%$
$\nu_m < \nu_{sa}$	$< 10.6 \cdot 10^{-2}$	$< 19.1 \cdot 10^{-2}$	> 0.3	$> 1.0 \cdot 10^{-2}$	$> 2.3 \cdot 10^{-1}$	$< 97\%$
Energy injection scenario where $p = 2.73 \pm 0.03$						
$\nu_c > \nu_{xrt}$, $k = 2$	>1.1	$< 6.6 \cdot 10^{-10}$	$> 1.2 \cdot 10^{3}$	>1.0	> 2.4	$< 77\%$
$\nu_c > \nu_{xrt}$, $k = 1.1$	$> 74.6 \cdot 10^{-2}$	$< 2.1 \cdot 10^{-9}$	$> 4.3 \cdot 10^{5}$	>0.8	> 3.4	$< 71\%$
$\nu_c > \nu_{xrt}$, $k = 0$	$> 75.2 \cdot 10^{-2}$	$< 2.2 \cdot 10^{-9}$	$> 1.2 \cdot 10^{7}$	>0.8	> 3.7	$< 69\%$

Table 1: Physical parameters for GS, DC and Energy injections models. $\bar{\varepsilon}_e = \varepsilon_e \times (|p-2|)/(p-1)$. For $k = 2$ we report the density in terms of A_*, where $A = \dot{M}/4\pi v_w = 5 \times 10^{11} A_*$ g cm^{-1} [16]. $\eta = E^{\gamma}_{iso}/(E^{\gamma}_{iso} + E_{iso})$. [17, 18]

4. Discussion and conclusions

We analysed the multi-wavelength observations of the afterglow of GRB 121024A. The combined GROND and XRT data allow us to measure with high accuracy the spectral slope in this energy regime, and therefore the electron index p. We describe our complete set of observations using two different models, where the break in the light curve marks either a jet break or the cessation of energy injection. The jet break model requires a hard electron spectrum with $p < 2$, a very low cooling break frequency [19] and a non-spreading jet [20,21]. The energy injection model does not require high efficiency values and is not in contradiction with Fermi acceleration predictions for p, but gives atypical values for some of the micro-physical and dynamical parameters.

Although no clear preferred model describing the observations of this GRB afterglow emerges, we are able to rule out some of the possible models suggested by the closure relations [22]. First, we rule out the spectral regime where $\nu_{\rm sa} < \nu_{\rm m}$ for the jet break model. In the GS scenario [14], it is ruled out because the spectral evolution will never cross that regime in the slow cooling phase and in the DC scenario [15] it is ruled out because the time when $\nu_{\rm m}$ crosses $\nu_{\rm sa}$ is before the time of the studied SED ($t = 109$ ks). Second, we rule out the energy injection model for the wind density profile $k = 2$ because $\bar{\epsilon}_{\rm e}$ has to be larger than one, which is not physically meaningful.

There are two possible models left describing the observations. First, energy injection model where we either take $k = 0$ (ISM) or fit $k = 1.1$ for the density profile. This model requires extremely high density values compared to theoretical expectations and previous measurements, and it also implies spherical outflow geometry. Second, the jet break model for the spectral regime where $\nu_{\rm m} < \nu_{\rm sa}$. This gives physically meaningful micro-physical and dynamical parameters, although it has some issues with the efficiency requirements, the position of the cooling break, and the hard electron spectrum. However, this is not the first GRB with these issues. Specifically, this is not the first GRB afterglow for which a hard electron spectrum has been inferred. Different treatments of hard spectra have been put forward in the literature. We have investigated two, and found to give reasonable and physically meaningful results. Finally, the linear polarisation observations [3] are in agreement with a jet break model where the linear polarisation jump is a direct result from the jet break. However, this type of transition in polarisation has not been investigated yet in the literature for energy injection breaks, which might lead to a similar effect.

The results presented here on GRB121024A show that broadband afterglow data from the X-ray to radio allow for a detailed analysis of the characteristic properties of the GRB afterglow synchrotron emission spectrum. Through our extensive data coverage we have been able to constrain the position of all synchrotron breaks, which in turn has allowed us to measure all the micro-physical and dynamical parameters of the GRB afterglow. This information is crucial to study further the GRB afterglow emission processes. Future continual coverage of the GRB afterglow with sensitive telescopes over a wide wavelength range and at multiple epochs will enable us to place strong constraints on the micro-physical parameters for a larger sample of GRBs, and allow us to e.g. investigate the evolution of these parameters.

Acknowledgements. KV acknowledges support by DFG grant SA 2001/2-1. H.v.E acknowledges support by the Alexander von Humboldt foundation. JG acknowledges support by the DFG cluster of excellence "Origin and Structure of the Universe" (www.universe-cluster.de). P.S. acknowledges support through the Sofja Kovalevskaja Award from the Alexander von Humboldt Foundation of Germany. Part of the funding for GROND (both hardware as well as personnel) was generously granted from the Leibniz-Prize to Prof. G. Hasinger (DFG grant HA 1850/28-1). This work made use of data supplied by the UK Swift Science Data Centre at the University of Leicester. APEX is operated by the Max-Planck-Institut für Radioastronomie, the European Southern Observatory, and the Onsala Space Observatory.

References

[1] P. Mészáros and M. J. Rees, Optical and Long-Wavelength Afterglow from Gamma-Ray Bursts, *Astrophys. J.*, **476** 232 (1997).

[2] N. R. Tanvir, J. P. U. Fynbo, et al., *GRB 121024A: VLT/X-shooter redshift*, *GRB Coordinates Network*, **13890** (2012).

[3] K. Wiersema, S. Covino, et al., *Circular polarization in the optical afterglow of GRB 121024A*, *Nature*, **509** 201 (2014).

[4] C. Pagani, S. D. Barthelmy, et al., GRB 121024A: Swift detection of a burst with an optical counterpart, *GRB Coordinates Network* **13886** (2012).

[5] P. A. Evans, A. P. Beardmore, et al., *Methods and results of an automatic analysis of a complete sample of Swift-XRT observations of GRBs*, *MNRAS*, **397** 1177 (2009).

[6] N. R. Butler and D. Kocevski, *X-Ray Hardness Evolution in GRB Afterglows and Flares: Late-Time GRB Activity without N_H Variations*, *Astrophys. J.*, **663** 407 (2007).

[7] J. Greiner, W. Bornemann, et al., *GROND a 7-Channel Imager*, *PASP*, **120** 405 (2008).

[8] F. Knust, P. Schady, and J. Greiner, *GRB 121024A: GROND detection of the Optical/NIR afterglow*, *GRB Coordinates Network* **13891** (2012).

[9] T. Krühler, A. Küpcü Yoldaş, et al., *The 2175 Å Dust Feature in a Gamma-Ray Burst Afterglow at Redshift 2.45*, *Astrophys. J.*, **685** 376 (2008).

[10] M. F. Skrutskie, R. M. Cutri,et al., *The Two Micron All Sky Survey (2MASS)*, *AJ*, **131** 1163 (2006).

[11] Siringo, G., Kreysa, E., et al., *The large apex bolometer camera laboca*, *Astron. & Astrophys.*, **497** 945 (2009).

[12] B. Zauderer, T. Laskar, and E. Berger, *GRB 121024A: CARMA 3mm detection*, *GRB Coordinates Network*, **13900**, (2012).

[13] T. Laskar, A. Zauderer, and E. Berger, GRB 121024A: EVLA detection, *GRB Coordinates Network* **13903** (2012).

[14] J. Granot and R. Sari, *The Shape of Spectral Breaks in Gamma-Ray Burst Afterglows*, *Astrophys. J.*, **568** 820 (2002).

[15] Z. G. Dai and K. S. Cheng, *Afterglow Emission from Highly Collimated Jets with Flat Electron Spectra: Application to the GRB 010222 Case?*, *Astrophys. J.*, **558** L109 (2001).

[16] R. A. Chevalier and Z.-Y. Li, *Wind Interaction Models for Gamma-Ray Burst Afterglows: The Case for Two Types of Progenitors*, *Astrophys. J.*, **536** 195 (2000).

[17] F. Daigne and R. Mochkovitch, *Gamma-ray bursts from internal shocks in a relativistic wind: temporal and spectral properties*, *MNRAS*, **296** 275 (1998).

[18] S. Kobayashi, T. Piran, and R. Sari, *Can Internal Shocks Produce the Variability in Gamma-Ray Bursts?*, *Astrophys. J.*, **490** 92 (1997).

[19] J. Greiner, T. Krühler, et al., *The nature of "dark" gamma-ray bursts*, *Astron. & Astrophys.*, **526** A30 (2011).

[20] F. De Colle, E. Ramirez-Ruiz, et al.,. *Simulations of Gamma-Ray Burst Jets in a Stratified External Medium: Dynamics, Afterglow Light Curves, Jet Breaks, and Radio Calorimetry*, *Astrophys. J.*, **751** 57 (2012).

[21] H. van Eerten, W. Zhang, and A. MacFadyen, *Off-axis Gamma-ray Burst Afterglow Modeling Based on a Two-dimensional Axisymmetric Hydrodynamics Simulation*, *Astrophys. J.*, **722** 235 (2010).

[22] J. L. Racusin, E. W. Liang, et al., *Jet Breaks and Energetics of Swift Gamma-Ray Burst X-Ray Afterglows*. *Astrophys. J.*, **698** 43 (2009).